

Control of electron transport related defects in *in situ* fabricated single wall carbon nanotube devices

Zhixian Zhou,^{a)} R. Jin, Gyula Eres, Alaska Subedi, and D. Mandrus

Materials Science and Technology Division, Oak Ridge National Laboratory, Oak Ridge, Tennessee 37831

(Received 8 May 2006; accepted 26 July 2006; published online 29 September 2006)

Metallic single wall carbon nanotube devices were characterized using low temperature transport measurements to study how the growth conditions affect defect formation in carbon nanotubes. Suspended carbon nanotube devices were grown *in situ* by a molecular beam growth method on a pair of catalyst islands located on opposing Au electrodes fabricated by electron beam lithography. The authors present experimental evidence that defect formation in carbon nanotubes, in addition to the well known growth temperature dependence, is also affected by the nature and the composition of the carbon growth gases. © 2006 American Institute of Physics. [DOI: 10.1063/1.2354450]

The intriguing electrical properties of carbon nanotubes (CNTs) stemming from their unique structure make them a promising candidate for nanometer scale electronic devices. For instance, field effect transistors (FETs) made of semiconducting single wall carbon nanotubes (SWCNTs) have demonstrated device properties surpassing those of state-of-the-art metal-oxide-semiconductor FETs.^{1–3} However, the application of CNTs as active elements in electronics also requires that the devices be reliably fabricated at predetermined locations on a substrate. A number of groups have fabricated CNT devices by *in situ* growth of CNTs electrically contacting opposing electrodes.^{4–8} However, little work has been done on the control of the defects in *in situ* fabricated SWCNT devices, even though the defect-induced disorder may significantly affect the electronic properties of SWCNTs.^{9,10} In this letter, we present a method that enables batch fabrication of SWCNT devices by directly growing individual SWCNTs on prefabricated Au electrodes, using a molecular beam.¹¹ We demonstrate that the defect level in the SWCNTs can be controlled during growth as characterized by low temperature transport measurements.

The CNT devices were fabricated on degenerately doped 4 in. Si wafers with 500 nm of thermal SiO₂ as schematically illustrated in Fig. 1(a). The electrodes were defined using electron beam lithography (EBL) followed by electron-gun assisted deposition of a 5 nm Ti adhesion layer and 200 nm of Au. Small catalyst islands consisting of 10 nm of Al and 1 nm of Fe were fabricated on top of the Au electrodes using a second EBL step and subsequent metal deposition. The substrate was heated to a temperature in a range from 650 to 825 °C in a vacuum chamber evacuated by a turbomolecular pump. During pregrowth heating, the Al layer melts and forms small clusters, which react with residual water in the chamber to form thermally and chemically stable Al₂O₃ clusters providing support for small particles of Fe₂O₃ that catalyze the growth of SWCNTs.¹¹ SWCNTs are grown by a molecular beam, consisting of a mixture of 0%–5% acetylene, 0%–10% methane, 10%–11% hydrogen, and the balance inert gas (helium or argon), generated by a high-pressure gas expansion through a 100 μm diameter nozzle orifice.¹¹ The gas molecules in the beam

impinge on the heated substrate and SWCNTs grow by heterogeneous surface reactions. The flux of carbon containing molecules was typically in the 10¹⁶ molecule/cm² range.¹¹

In our CNT devices, individual SWCNTs are routinely found to bridge the opposing electrodes. Figure 1(b) depicts a typical example of a suspended individual SWCNT electrically contacting two Au electrodes separated by 500 nm. To determine the diameter distribution of the SWCNTs, we performed atomic force microscopy measurements on substrate-supported SWCNTs grown under identical conditions as the suspended ones, and found that the diameters of the vast majority of the SWCNTs were in the 1–2 nm range, indicating individual SWCNTs. Electrical transport measurements were conducted on the as-grown samples in a temperature range from room temperature (RT) to 300 mK using the degenerately doped substrate as a back gate. Both metallic and semiconducting nanotubes were observed based on the gate dependence of the conductance at RT. In this letter, we focus only on metallic SWCNTs, since metallic tubes are relatively insensitive to long range disorder.¹⁰ While both high defect

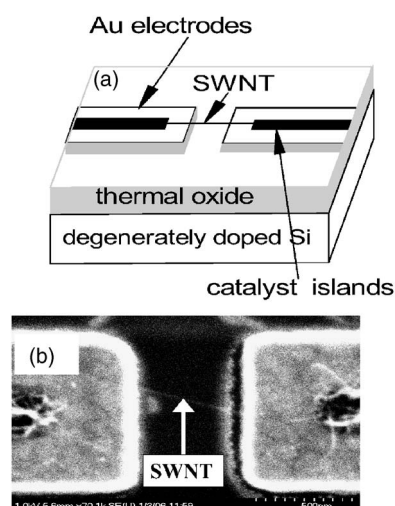


FIG. 1. (a) Schematic diagram of the SWCNT device, where Au electrodes are defined by EBL followed by deposition of 5 nm of Ti and 200 nm of Au and catalyst islands are fabricated by a second EBL step and subsequent deposition of 10 nm of Al and 1 nm of Fe. (b) Scanning electron microscope image showing an as-grown SWCNT suspended between two Au electrodes as indicated by the arrow; the Au electrodes are separated by approximately 500 nm.

^{a)} Author to whom correspondence should be addressed, electronic mail: zhouz@ornl.gov

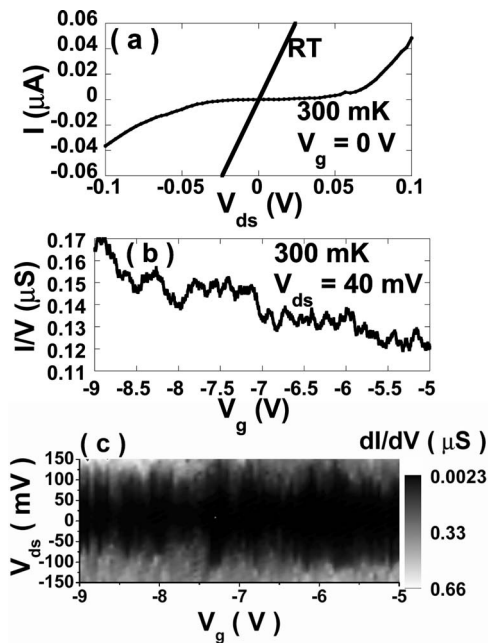


FIG. 2. A representative high defect SWCNT device. (a) I - V curves measured at room temperature and 300 mK for $V_g=0$. (b) I/V_{ds} as a function of gate voltage V_g for $T=300$ mK and $V_{ds}=40$ mV. (c) Differential conductance as a function of bias and gate voltage for $T=300$ mK measured by superimposing a small ac voltage $V_{ac}=0.5$ mV ($f=171$ Hz) on top of V_{ds} .

and low defect metallic SWCNTs show similar linear I - V dependence and are indistinguishable at RT, they exhibit substantially different characteristics at low temperatures.

Figure 2 shows the transport data measured on a SWCNT device grown at 650°C using 5% acetylene as the only carbon source. The I - V curve of this device is linear at RT, and the resistance is around 400 k Ω . The linear I - V and the lack of gate dependence in RT conductance are characteristics of metallic SWCNTs. However, with decreasing temperature, a near-zero conductance gap of $-50 < V_{ds} < 50$ mV emerges, that is almost an order of magnitude larger than that expected for the Coulomb blockade (CB) effect for a single quantum dot (QD).¹² The conductance (I/V_{ds}) of the device measured at $V_{ds}=40$ mV and $T=300$ mK exhibits irregular oscillations, as opposed to regular CB peaks commonly observed in single QD. To determine the origin as well as the energy scale of these irregular oscillations, differential conductance (dI/dV_{ds}) as a function of V_g and V_{ds} was measured on the same device at 300 mK by applying a dc+ac voltage, $V=V_{ds}+V_{ac}$ (with $V_{ac}=0.5$ mV at $f=171$ Hz), and the results are shown in Fig. 2(c). The CB ‘‘diamonds’’ in Fig. 2(c) are highly irregular and do not close, leaving a near-zero conductance region for $V_{ds} < 50$ mV, in contrast to regular closed CB diamonds expected in single QDs.^{12,13} In addition, the single electron charging energy extracted from Fig. 2(c) is approximately 100 meV, almost an order of magnitude larger than that of a SWCNT QD with the same length (~ 500 nm), indicating that the device in Fig. 2(c) acts like multiple (approximately ten) QDs connected in series.¹⁰ Similar transport behavior was exhibited by all devices grown with acetylene.

In contrast, SWCNTs grown at 825°C with the addition of 7% methane to the 5% acetylene mixture are nearly defect-free, showing regular CB peaks in all five metallic devices measured. The examples shown in Fig. 3 correspond to devices with ~ 500 nm long SWCNTs between the elec-

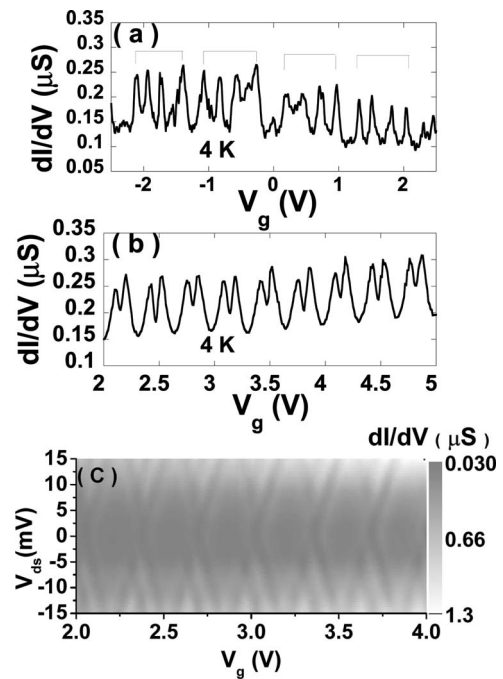


FIG. 3. Differential conductance as a function of gate voltage (dI/dV vs V_g) of two low defect SWCNT devices measured at $T=4$ K and under a small ac voltage between the drain and source, $V_{ac}=0.5$ mV ($f=171$ Hz). (a) Four-peak shell structure characteristic of a SWCNT quantum dot. (b) In this SWCNT device, interdot tunneling splits each of the otherwise equally spaced Coulomb blockade peaks into two peaks in a weakly coupled double quantum dot system. (c) Differential conductance as a function of bias and gate voltage of the device in (b) at 4 K and under $V_{ac}=0.5$ mV ($f=171$ Hz).

trodes. The device in Fig. 3(a) displays four-peak structures corresponding to ‘‘shell filling’’ of longitudinally quantized states in the SWCNT,¹² indicating that the SWCNT in this device is nearly defect-free. In the second example, Coulomb peaks are overall equally spaced in gate voltage V_g as shown in Fig. 3(b). However, each peak also clearly splits into two peaks with a constant separation. Similar behavior has been observed in GaAs/ $\text{Al}_x\text{Ga}_{1-x}$ based double QD systems, where the splitting of the otherwise equally spaced peaks is attributed to interdot tunneling between two QDs with equal gate capacitance.^{14,15} Mason *et al.* recently reported the observation of double QDs in their CNT devices fabricated using a different method.¹⁶ In our case, the double QD is most likely created by a defect near the middle of the device breaking the SWCNT between the electrodes into two weakly coupled dots of nearly equal length. The transport spectroscopy of the device shown in Fig. 3(c) exhibits periodic CB diamonds with a single electron charging energy of $E_c \sim 18$ meV, approximately twice that of a single QD with the same length scale and configuration, further demonstrating that the two quantum dots are nearly identical and thus have the same periodicity in both V_{ds} and V_g .

The range of growth parameters explored in this study along with the number of samples characterized by low temperature transport measurements are summarized in Table I. Gas mixtures containing acetylene alone as the carbon source molecule easily produced SWCNT bridging the electrodes. In contrast, a gas mixture containing methane alone produced no CNTs likely because of the low carbon yield of methane. However, the SWCNTs grown using acetylene contained defects that could not be eliminated by increasing the

TABLE I. Range of growth parameters, the number of samples (in parentheses), and the corresponding electron transport related defect levels of SWCNT devices.

	5% C ₂ H ₂ , 10% H ₂ , and 85% He	5% C ₂ H ₂ , 7% CH ₄ , 11% H ₂ , and 77% Ar
650 °C	High defect (5)	High defect (7)
825 °C	High defect (11)	Low defect (5)

growth temperature. The most notable result of this study is that the addition of methane to the acetylene gas mixture consistently produced low defect or nearly defect-free SWCNTs, but only at high growth temperatures. The observation that the nature (and the composition) of carbon containing source molecules affects defect formation in SWCNTs suggests that the molecular structure of carbon containing molecules plays a specific role in the formation of carbon networks. We speculate that the presence of C–C bonds in acetylene facilitates efficient nucleation of the SWCNTs,¹¹ and methane by addition of single carbon atom fragments helps to heal defects in the SWCNTs.

In summary, we have developed a method to fabricate SWCNT devices by using e-beam lithography to pattern catalyst islands on Au electrodes, followed by molecular beam induced growth of SWCNTs electrically contacting opposing electrodes. Electrical transport and transport spectroscopy measurements are used to study the defect related transport behavior of as-grown SWCNTs, revealing multiple dots in series and single quantum dot or double dots in high and low defect SWCNTs, respectively. We presented experimental evidence that the presence of defects in as-grown SWCNTs depends not just on the substrate temperature but also on the nature and the composition of the feedstock gas mixture.

The authors would like to thank Pam Fleming for technical assistance. Research was sponsored by the Division of Materials Sciences and Engineering, Office of Basic Energy Sciences, U.S. Department of Energy, under Contract No. DE-AC05-00OR22725 with Oak Ridge National Laboratory, managed and operated by UT-Battelle, LLC.

- ¹W. Kim, H. C. Choi, M. Shim, Y. Li, D. Wang, and H. Dai, *Nano Lett.* **2**, 703 (2002).
- ²M. S. Fuhrer, B. M. Kim, T. Durkop, and T. Brintlinger, *Nano Lett.* **2**, 755 (2002).
- ³S. Rosenblatt, Y. Yalsh, J. Park, J. Gore, V. Sazonova, and P. L. McEuen, *Nano Lett.* **2**, 869 (2002).
- ⁴Y. Y. Wei and G. Eres, *Appl. Phys. Lett.* **76**, 3759 (2000).
- ⁵N. R. Franklin, Q. Wang, T. W. Tombler, A. Javey, M. Shim, and H. Dai, *Appl. Phys. Lett.* **81**, 913 (2002).
- ⁶J. Cao, Q. Wang, and H. Dai, *Nat. Mater.* **4**, 745 (2005).
- ⁷R. Y. Zhang, I. Amlani, J. Baker, J. Tresek, R. K. Tsui, and P. Fejes, *Nano Lett.* **3**, 731 (2003).
- ⁸H. B. Peng, T. G. Ristorph, G. M. Schurmann, G. M. King, J. Yoon, V. Narayanamurti, and J. A. Golovchenko, *Appl. Phys. Lett.* **83**, 4238 (2003).
- ⁹M. Bockrath, W. Liang, D. Bozovic, J. H. Hafner, C. M. Lieber, M. Tinkham, and H. Park, *Science* **291**, 283 (2001).
- ¹⁰P. L. McEuen, M. Bockrath, D. H. Cobden, Y.-G. Yoon, and S. G. Louie, *Phys. Rev. Lett.* **83**, 5098 (1999).
- ¹¹G. Eres, A. A. Kinkhabwala, H. T. Cui, D. B. Geohegan, A. A. Puzos, and D. H. Lowndes, *J. Phys. Chem. B* **109**, 16684 (2005).
- ¹²S. Sapmaz, P. Jarillo-Herrero, J. Kong, C. Dekker, L. P. Kouwenhoven, and H. S. J. van der Zant, *Phys. Rev. B* **71**, 153402 (2005).
- ¹³P. Jarillo-Herrero, S. Sapmaz, C. Dekker, L. P. Kouwenhoven, and H. S. J. van der Zant, *Nature (London)* **429**, 389 (2004).
- ¹⁴F. R. Waugh, M. J. Berry, C. H. Crouch, C. Livermore, D. J. Mar, R. M. Westervelt, K. L. Campman, and A. C. Gossard, *Phys. Rev. B* **53**, 1413 (1996).
- ¹⁵F. R. Waugh, M. J. Berry, D. J. Mar, R. M. Westervelt, K. L. Campman, and A. C. Gossard, *Phys. Rev. Lett.* **75**, 705 (1995).
- ¹⁶N. Mason, M. J. Biercuk, and C. M. Marcus, *Science* **303**, 655 (2004).